



OPEN

High variability of atmospheric mercury in the summertime boundary layer through the central Arctic Ocean

SUBJECT AREAS:

ENVIRONMENTAL
CHEMISTRY

ATMOSPHERIC SCIENCE

OCEAN SCIENCES

Juan Yu¹, Zhouqing Xie¹, Hui Kang¹, Zheng Li¹, Chen Sun¹, Lingen Bian² & Pengfei Zhang^{1,3}Received
26 March 2014Accepted
30 July 2014Published
15 August 2014Correspondence and
requests for materials
should be addressed to
Z.Q.X. (zqxie@ustc.
edu.cn)

¹Institute of Polar Environment, School of Earth and Space Sciences, University of Science and Technology of China, Hefei 230026, China, ²Chinese Academy of Meteorological Sciences, Beijing 100081, China, ³Department of Earth and Atmospheric Sciences, City College of New York, New York, NY 10031, USA.

The biogeochemical cycles of mercury in the Arctic springtime have been intensively investigated due to mercury being rapidly removed from the atmosphere. However, the behavior of mercury in the Arctic summertime is still poorly understood. Here we report the characteristics of total gaseous mercury (TGM) concentrations through the central Arctic Ocean from July to September, 2012. The TGM concentrations varied considerably (from 0.15 ng/m³ to 4.58 ng/m³), and displayed a normal distribution with an average of 1.23 ± 0.61 ng/m³. The highest frequency range was 1.0–1.5 ng/m³, lower than previously reported background values in the Northern Hemisphere. Inhomogeneous distributions were observed over the Arctic Ocean due to the effect of sea ice melt and/or runoff. A lower level of TGM was found in July than in September, potentially because ocean emission was outweighed by chemical loss.

Atmospheric mercury is an atmospheric pollutant with two main sources: anthropogenic and natural. Commonly, anthropogenic sources include coal combustion, waste incineration, metal smelting, refining and manufacturing, and gold mining. Natural sources include emissions from oceans, surface soils, water bodies (both fresh and salty water), vegetation surfaces, wild fires, crustal out-gassing, volcanoes, and geothermal sources^{1,2}. Due to its relatively high vapor pressure, low solubility and relatively long atmospheric residence time (about 1 year), mercury can be globally transported³, even to remote areas such as the Arctic⁴ and Antarctica⁵. During its long-range transport, gaseous elemental mercury can deposit on surfaces through both wet and dry processes acting on Hg(II) and Hg(p) species¹. Once deposited into the environment, inorganic mercury species are likely to convert into highly toxic methyl mercury (MeHg) species, which are then enriched in the aquatic food chain and may pose threats to human health eventually¹.

At present, the seasonality of atmospheric mercury based on the long term site observation is obvious in the Arctic. The pattern of variability for atmospheric mercury in the Arctic area presented the spring minimum and summer maximum^{6,7}. During the polar spring, the depletion of Hg⁰ correlated with the loss of O₃⁸. This depletion event was initiated by halogen species originating from sea salt linked to sea ice⁹ or snow on the sea ice¹⁰ after polar sunrise in the Arctic springtime¹¹. The deposited mercury in the Arctic can undergo both reduction and oxidation processes in the snow and some may be re-emitted to the atmosphere¹². However, the variable characteristics of atmospheric mercury in the Arctic summer, especially over the Arctic Ocean, are poorly understood. It is known that oceans play an important role in the cycle of global mercury because they can serve as sources or sinks for atmospheric mercury through air-sea exchange^{13,14}. Modeling work showed that the maximum mercury in Arctic summer may be driven by river sources based upon a few site observations¹⁵. The *Beringia* 2005 expedition over the Arctic Ocean in the Northwest passage presented a rapid increase of mercury in air when entering the ice-covered waters⁴. As the Arctic Ocean has undergone a shift in decreasing sea ice extent in summer, the effect of this shift on the cycle of atmospheric mercury remains unknown.

During the 5th Chinese National Arctic Research Expedition (CHINARE 2012), the Chinese vessel *Xuelong* passed through the Northeast Passage and the central Arctic Ocean. Moreover, in CHINARE 2010 *Xuelong* cruised the same track in the Chukchi Sea. This provides opportunity to investigate the spatial and temporal distribution of atmospheric mercury over the Arctic Ocean and to examine the complex interrelations.

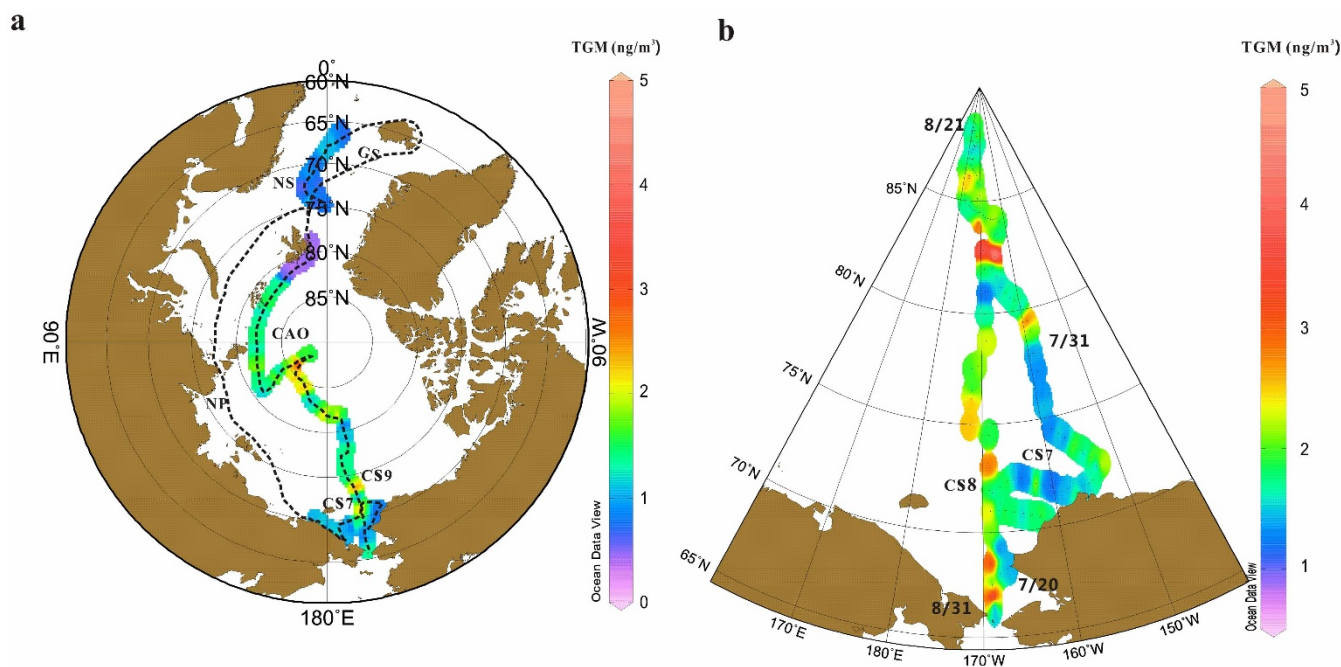


Figure 1 | Spatial distribution of TGM in air (ng/m^3) along the cruise paths during CHINARE 2012(a) and 2010(b), respectively, generated by Ocean Data View 4.0. The cruise dates were UTC time. The dashed line without color means the period without data. Base map is from Ocean Data View 4.0.

Results

General observation. Figure 1 shows the TGM concentrations in the marine boundary layer (MBL) during both CHINARE 2012 and CHINARE 2010 along the cruise paths. During CHINARE 2012, the cruise started on July 18th in the Chukchi Sea, passed through the Northeast Passage, arrived at Ice Island, then returned to the Chukchi Sea on September 8th through the central Arctic. The instrument was turned off when the ship passed through the Northeast Passage near the Russia coast due to political reasons. The TGM concentrations for the sites around the Ice Island but outside the Arctic Ocean were not considered in this study. The instrument was also turned off over the Greenland Sea due to the carrier gas for instrument being exhausted. Details of the cruise legs during CHINARE 2012 are shown in Table S1. For CHINARE 2010, the cruise started on July 20th in the Chukchi Sea, reached the central Arctic Ocean and then returned to the Chukchi Sea on August 31th. For CHINARE 2012, the concentrations varied considerably from $0.15 \text{ ng}/\text{m}^3$ to $4.58 \text{ ng}/\text{m}^3$, with an average of $1.23 \pm 0.61 \text{ ng}/\text{m}^3$ (median: $1.15 \text{ ng}/\text{m}^3$). The average is lower than the reported data over the western Arctic Ocean in 2005 ($1.72 \pm 0.35 \text{ ng}/\text{m}^3$)⁴. However, it is somewhat higher than the average over the North Atlantic Ocean in 2008 (about $1.15 \text{ ng}/\text{m}^3$) and 2009 (about $1.12 \text{ ng}/\text{m}^3$)². TGM concentrations displayed an inhomogeneous distribution over the oceans, similar to the results obtained during the expedition of *Galathea 3* cruise¹⁶, which covered the North Atlantic Ocean etc. The spatial distribution of TGM over the Arctic Ocean is notably in agreement with the recent observation of higher Hg in biota in the western Arctic than in the east^{17,18}. The frequency distribution of TGM concentrations is given in Figure 2a, and the Kolmogorov-Smirnov test suggested a normal distribution ($P < 0.001$). The highest frequency is in the range from 1.0 to $1.5 \text{ ng}/\text{m}^3$.

For CHINARE 2010, the TGM concentrations ranged from 0.73 to $4.78 \text{ ng}/\text{m}^3$, with an average of $1.81 \pm 0.45 \text{ ng}/\text{m}^3$ (median: $1.72 \text{ ng}/\text{m}^3$). Again, Kolmogorov-Smirnov test suggested a normal TGM distribution ($P < 0.001$). The highest frequency range was 1.6 – $1.8 \text{ ng}/\text{m}^3$ (Figure 2b). Approximately 30% data were below $1.5 \text{ ng}/\text{m}^3$ during CHINARE 2010, while the frequency increased

up to approximately 80% during CHINARE 2012. It implies that many observations over the Arctic Ocean fell outside of the range of earlier reported background value (1.5 – $1.7 \text{ ng}/\text{m}^3$) in the Northern Hemisphere¹⁹.

Regional characteristics. As shown in Figure 3a and Figure 3b, TGM concentrations show different characteristics at different locations along the cruises. To better interpret the data we divided the cruises into several geographical legs. During CHINARE 2010, the cruise in the Chukchi Sea was named CS7-2010 (Chukchi Sea in July) and CS8-2010 (Chukchi Sea in August), respectively. During CHINARE 2012 the cruise path was divided into 4 legs, namely CS7 (Chukchi Sea in July), NS (Norwegian Sea), CAO (central Arctic Ocean) and CS9 (Chukchi Sea in September) according to the status of sea ice and ocean basin. The TGM concentrations decreased when the ship passed NS to CAO, and then abruptly increased in the CAO leg (Figure 3a). According to the report of 2012 Chinese Arctic Research Expedition, both the NS leg and the beginning of the CAO leg were in open water whereas the later part of the CAO leg was in an ice-covered region. In the ice-covered region over the CAO leg, air pressure and RH increased, while temperature decreased (Table S1). TGM abruptly increased when the ship entering the ice-covered region (Figure 3a). This phenomenon was also observed during CHINARE 2010 (Figure 3b) and the *Beringia* 2005 expedition through the Northwest passage of the Arctic Ocean⁴ and the Atlantic Ocean²⁰. For the NS leg, the average TGM value was $0.81 \pm 0.26 \text{ ng}/\text{m}^3$, which was relatively low compared to the other oceans (see Table S1). Near the leg NS, low TGM (approximately $1.1 \text{ ng}/\text{m}^3$), was also observed over the northern Atlantic Ocean in 2008 and 2009². For the legs CS7 and CS9, TGM of CS7 ($1.17 \pm 0.38 \text{ ng}/\text{m}^3$) was obviously lower than that of CS9 ($1.51 \pm 0.79 \text{ ng}/\text{m}^3$). This was different from the land based observation around the Arctic Ocean, where a decreasing trend from July to September was reported¹⁵. Measurements of TGM over the Chukchi Sea were also performed during CHINARE 2010. Monthly variations were also found in the 2010 cruise, i.e., the average TGM of CS8-2010 ($2.22 \pm 0.45 \text{ ng}/\text{m}^3$) was higher than that of CS7-2010 ($1.60 \pm 0.34 \text{ ng}/\text{m}^3$).

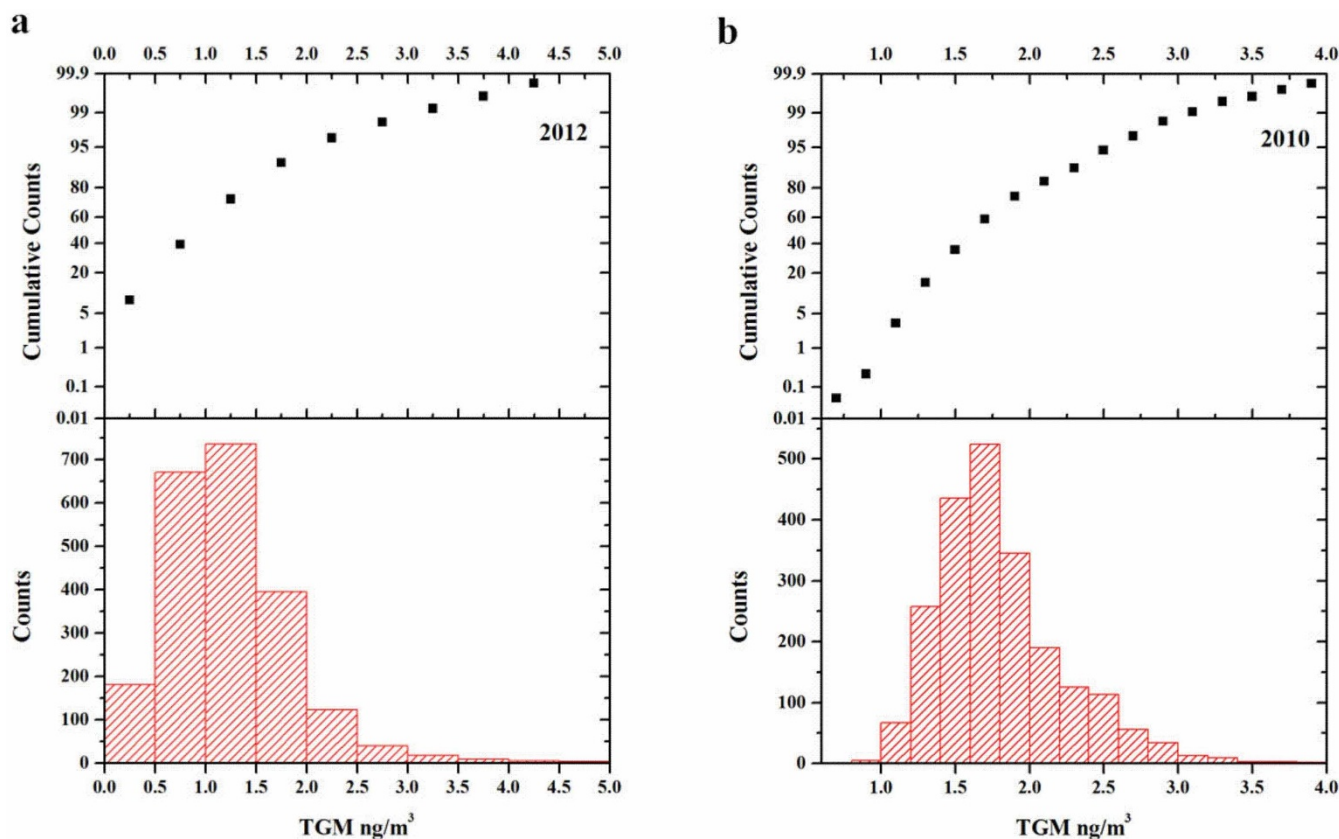


Figure 2 | Frequency distributions of TGM concentrations during CHINARE 2012(a) and 2010(b).

Discussion

Role of sea ice. Relatively high TGM concentrations were observed when the ship passed through the ice-covered region over the CAO leg, implying that sea ice may have played an important role on the spatial distributions of TGM. It was previously reported that relatively high dissolved gaseous mercury (DGM) concentration was found under the sea ice²¹. During the summer of 2012, the Arctic sea ice area decreased to a new record low²², and therefore may have enhanced the air-sea exchange. To examine the effect of sea ice, time series TGM data were compared with the distribution of salinity as ice melting will dilute the salinity of seawater²³ (Figure 4a and 4b). A statistical analysis yielded a negative correlation between TGM and salinity over the ice-covered region ($R = -0.3$, $P < 0.0001$), confirming that ice melting would enhance TGM concentrations over this region. It has been reported that a relatively high value of mercury was observed in the multiyear ice, especially in the topmost layer and the bottom ice layer²⁴. As sea ice starts to melt, mercury in the ice is released into seawater. The reemission of mercury to the atmosphere can be triggered by sunlight when snow or ice melts²⁵. In addition, the primary production of microorganisms may control inorganic mercury reduction in the surface water²⁶, acting as a potential source for the atmospheric mercury. Sea ice is a physical barrier to delay the evasion of DGM from the ocean to the atmosphere⁴. When a ship breaks sea ice, gaseous mercury can be emitted into the atmosphere. It is noted that the Chukchi Sea in July and August was covered with floating sea ice during CHINARE 2010. It has been reported that the Chukchi Sea was mainly influenced by the ice-melting water during this period (Table S2). Changes in sea ice from July to September also indicated that the melting sea ice in both legs CS7 and CS8 was mainly first-year ice (Figure S2). Therefore, the melting of sea ice cannot explain the differences of TGM concentrations in legs CS8-2010 and CS7-2010. Other potential factors are further discussed below.

Role of runoff. While sea ice melting may affect TGM concentrations, simulations suggested that runoff may be the dominant source of mercury to the Arctic Ocean in summer¹⁵. Although both sea ice melting and/or river runoff can dilute the salinity, changes in salinity in the Chukchi Sea would have been controlled by runoff as the Chukchi Sea was less ice-covered during the sampling period of 2012 (Figure S3). The role of runoff on the distribution of TGM includes two aspects: 1) runoff brings a high level of mercury²⁷ and hence enhance DGM in seawater; 2) runoff brings a high level of DOM which will reduce Hg^{2+} into gaseous mercury²⁸. Changes in TGM, salinity, and CDOM in July, 2012 in the Chukchi Sea are shown in Figure 4a, 4b and 4d, respectively. TGM concentrations were positively related to CDOM (cf Fig. 4a and 4d, data within the red rectangle), but were negatively related to salinity (cf Fig. 4a and 4b) and carbon monoxide (CO) (cf Fig. 4a and 4c). Low CO concentrations indicated that the high TGM concentrations were not influenced by atmospheric anthropogenic sources²⁹. Pegau showed that most of the sea ice contained relatively low CDOM concentrations³⁰. The relative high CDOM in the Chukchi Sea was thus ascribed to the runoff. In fact, it was also reported that CDOM from the river runoff dominated the entire Western Arctic Ocean³¹. CDOM represented a significant part of the DOM (up to 60%)³², implying that the content of CDOM can be used as a proxy of DOM to a certain degree. Many experiments showed that Hg^{2+} reduction is correlated with the DOM content²⁸. Mercury reduction by DOM includes two processes. The first was the direct reduction of reactive mercury by transferring ligand-metal charges³³. The second was the photolysis of DOM by forming reactive intermediate reductants³⁴. This may explain why TGM was observed to increase in corresponding to the enhanced CDOM and low salinity in Chukchi Sea (Figure 4a and 4d). However, a relatively high CDOM corresponding with low TGM concentrations was observed in the Norwegian Sea (Figure 4a and 4d). A

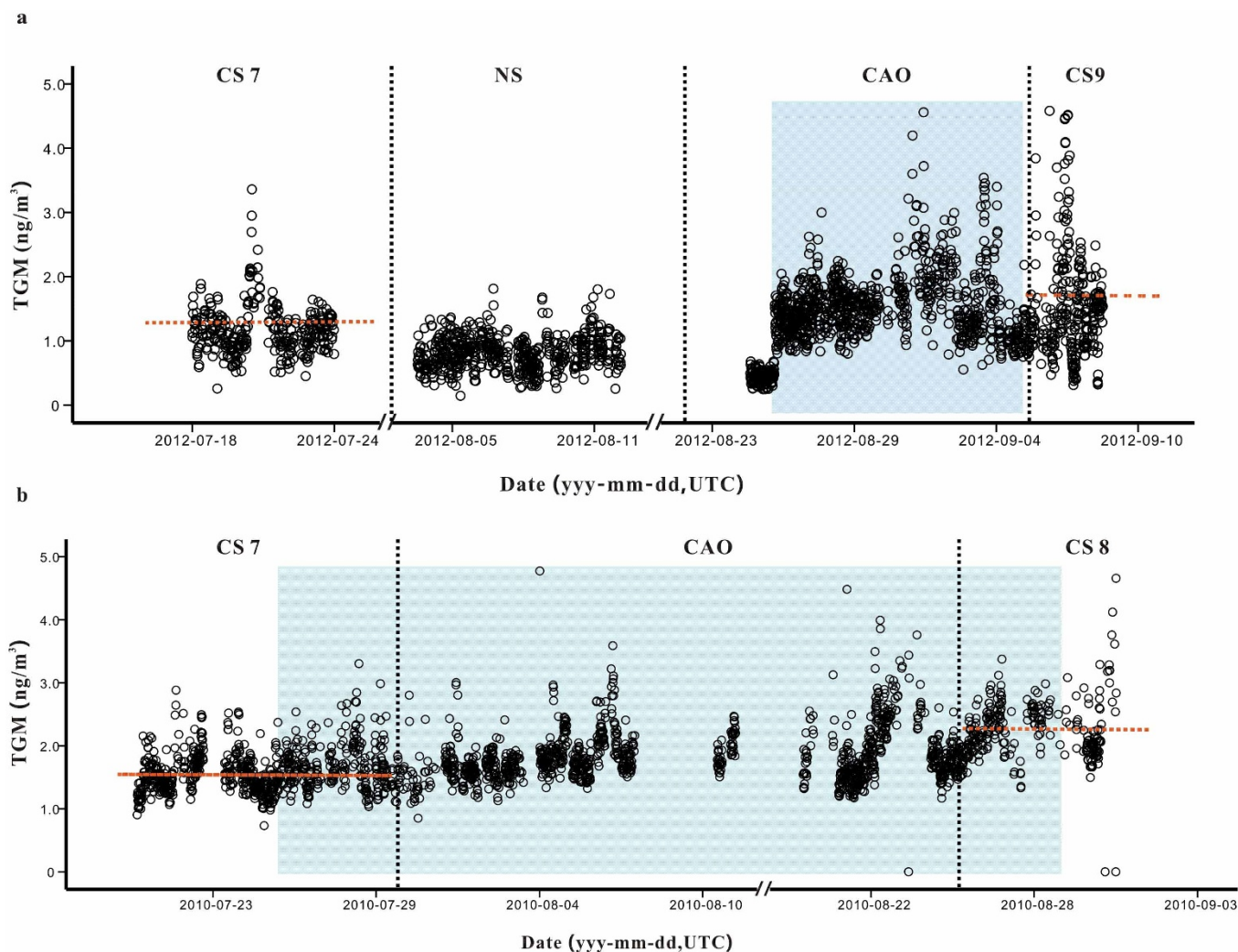


Figure 3 | Time series of atmospheric mercury concentrations along the cruise paths during CHINARE 2012(a) and 2010(b), respectively. The passage through ice-covered region is shaded in blue. The different legs are separated by the black dashed lines. The average TGM over the Chukchi Sea is indicated by the red dashed lines.

high salinity with no obvious decreasing trend indicated that this region was not impacted by runoff and hence no extra mercury was derived from runoff. It has been reported that in the Eurasian Basin the surface layer of the Arctic Ocean is mainly dominated by Atlantic Ocean³⁵, which maintains the high salinity in the Norwegian Sea. Mercury in the north Atlantic Ocean was low³⁶ and there was no DGM input from runoff. Therefore, TGM in the NS leg was low.

Role of chemical loss. River runoff cannot explain higher TGM in CS9 during CHINARE 2012, and higher TGM in CS8-2010 than in CS7 during CHINARE 2010. As the role of runoff and/or sea ice melting diminishes or ceases in Mid-August^{15,37}, emission of gaseous mercury may decrease accordingly. On the other hand, the air masses in September 2012 and August 2010 over the Chukchi Sea were from the Arctic Ocean rather than the continental source (Figure S4, Table S1), implying that long-range transport of continental sources is negligible. Consequently, we hypothesize that this summer monthly variation over the Chukchi Sea (opposite to land observations) may be due to less chemical loss from July to September. It is well known that mercury can be rapidly oxidized by halogen species after polar sunrise in the Arctic springtime¹¹. However, it is still unclear whether there is chemical loss in the Arctic summertime. Braking waves and sea spray were found to be the source of halogen in the atmosphere³⁸. Sea-salt

bromide can form Br₂ and BrCl and then photolyze to produce atomic Br and Cl under the daylight³⁸, implying that mercury may be oxidized by the halogens and/or other radicals during the Arctic summer. As chemical loss processes normally correlate with sunlight conditions, the change in sunlight intensity with TGM was investigated. As shown in Figure 5, the low TGM was correlated to the high sunlight intensity. In addition, the sunlight intensity was clearly decreasing from July to September both in 2012 and 2010 (see Figure S5a and S5b). Generally, high sunlight intensity will increase the boundary layer height and hence TGM may be diluted. However, the boundary layer was relatively stable over the surface of the Arctic Ocean and the vertical temperature change was minimal from July to September³⁹. An inversion layer was observed over the surface Ocean during the cruise in 2010 according to the report of 2010 CHINARE⁴⁰. The decreasing TGM concentrations from July to September thus cannot be explained by the boundary layer height. This implicates that chemical loss potentially exists in summer, and this loss will decrease from July to September. To further confirm whether chemical loss has occurred, changes in both TGM and CO were compared. A positive correlation between TGM and CO was observed ($R = 0.29, P < 0.0001$). As shown in Figure 2a and 2c, most of CO concentrations were below 150 parts per billion by volume (ppbv) and displayed an increasing trend from July to September. Because the background CO concentration in remote marine

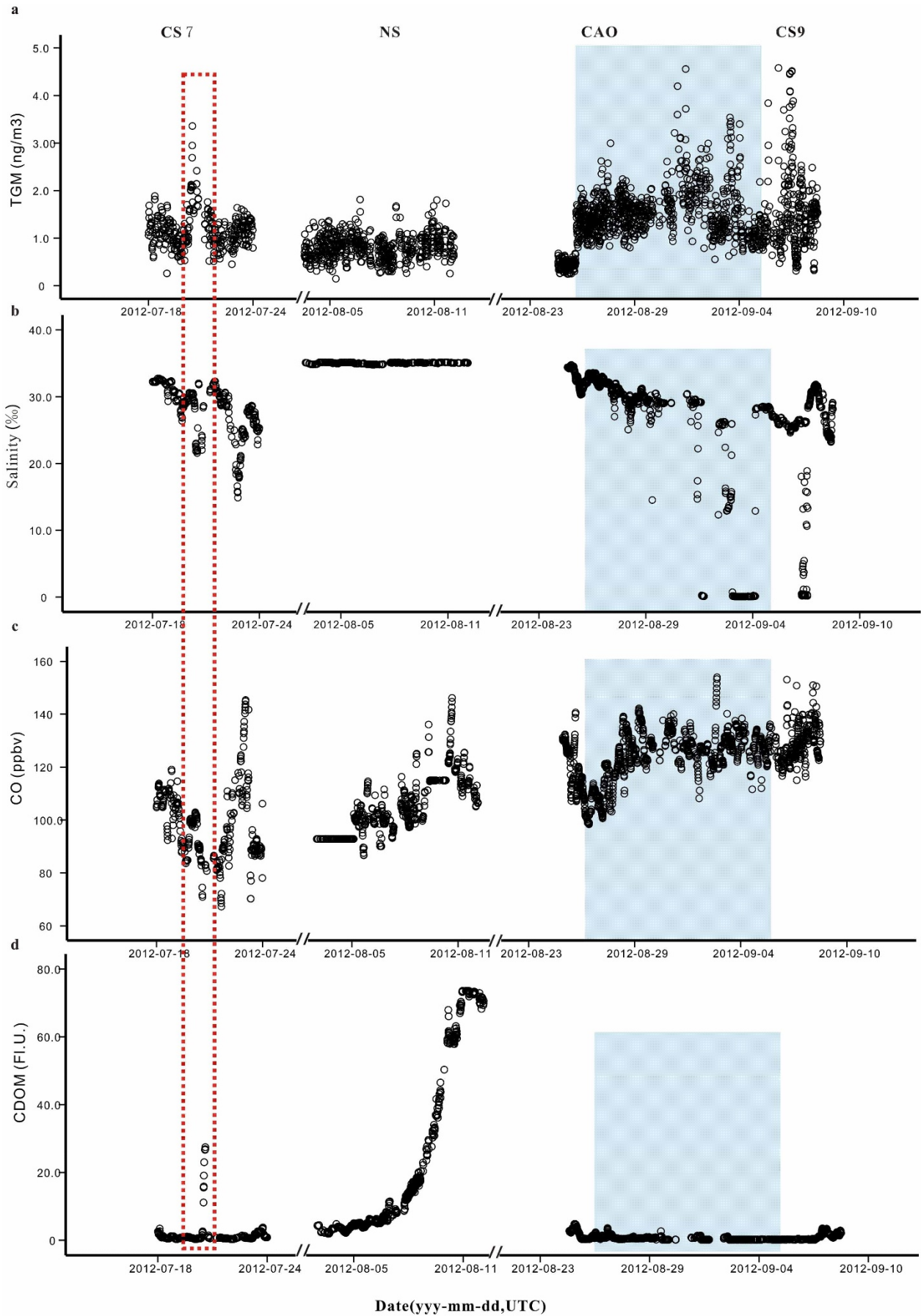


Figure 4 | Time series of TGM (a), carbon monoxide (CO) (b), salinity (c) and colored dissolved organic matter (CDOM) (d) along the cruise paths during CHINARE 2012. The passage through ice-covered region is shaded in blue.

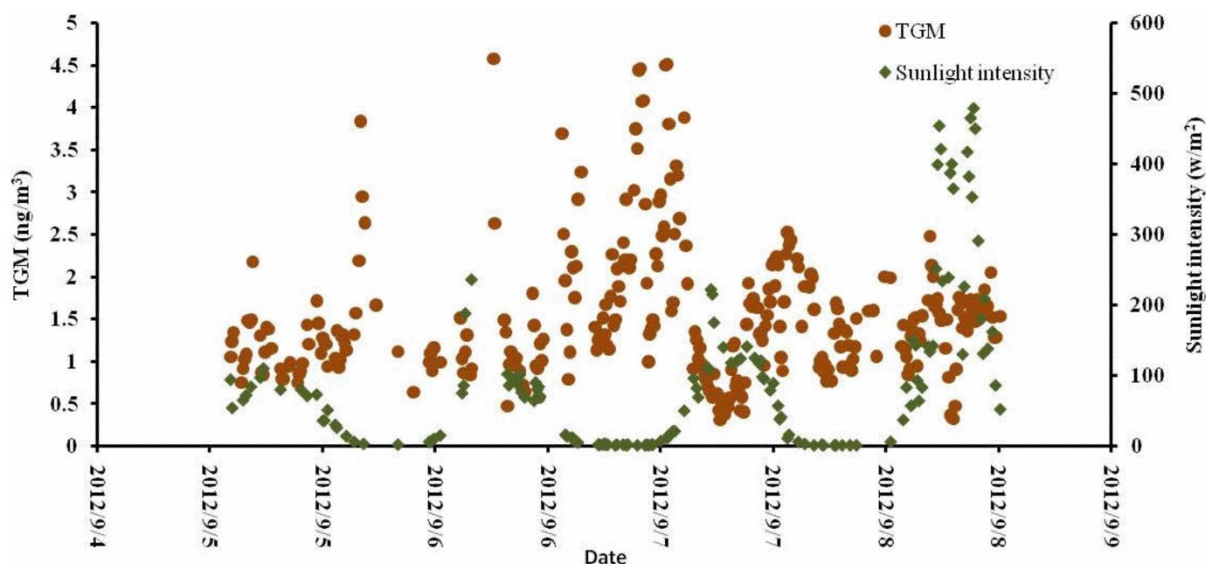


Figure 5 | An example of relationship between TGM and sunlight intensity.

environment is mostly below 150 ppbv^{41,42}, such monthly change should reflect CO background change in the Arctic Ocean. In fact, our observation of CO is in agreement with a previous report⁴¹. CO usually has a summer minimum largely due to the chemical oxidation by hydroxyl radical OH⁴³ and then increases with decreasing oxidation³⁸. As the change in mercury is similar to the destruction of CO by OH radicals, the chemical loss of mercury in summer should be further investigated.

Experimental Methods

The data over the Arctic Ocean were collected on the Chinese Research Vessel (R/V) *Xuelong* during CHINARE 2010 and CHINARE 2012, respectively. The cruise paths for CHINARE 2010 and CHINARE 2012 are shown in Figure 1a and 1b, respectively. Total gaseous mercury (TGM) measurements with 5-min resolution were carried out onboard by an automatic Mercury Vapor Analyzer (model 2537B, Tekran Inc., Toronto, Canada). The Tekran analyzer traps mercury from the air by amalgamating it on a gold cartridge, and the mercury is thermally desorbed from the gold cartridge and then detected by using cold vapor atomic fluorescence spectroscopy (CVAFS). The two gold cartridges ('A' and 'B') in parallel flow path were cycled with one in the sampling state and the other in the thermally desorbed state. During the sampling period, air flowed at a rate of 1.0 or 1.5 L/min through a 0.45 μm PTFE filter in the front of the inlet to prevent sea salt aerosols. The Tekran instrument was automatically recalibrated every 24 h by its internal permeation source. The detection limit is lower than 0.1 ng/m^3 in the operation mode. Manual calibrations by using a saturated mercury vapor standard injections were made before and after the field campaign. The relative percent differences between automated and manual calibrations were less than 2%, and the relative differences of the duplicate injections were less than 2%. More details on the measurement can be found in our previous publication⁷.

Ancillary data including trace gases, meteorological data and hydrologic data were simultaneously measured. Surface level O₃ mixing ratios were measured continuously using an O₃ analyzer (EC9810A, Australia), which combines microprocessor control with ultraviolet (UV) photometry^{44,45}. It was operated with an integration time of three minutes and one minute during CHINARE 2010 and CHINARE 2012, respectively. The detection limit was 0.5 ppb at a sampling rate of 0.5 L/min. Surface level CO mixing ratios were analyzed by COEC9830 monitors at a sampling rate of 1 L/min. Meteorological/hydrologic and GPS data with ten min-averaged value including wind direction, wind speed, air pressure (P), relative humidity (RH), atmospheric temperature (AT), sunlight intensity, color dissolved organic matter (CDOM), salinity, ship direction and ship speed were obtained from the ship's monitoring system.

The raw sampling data of TGM, O₃, CO and meteorological/hydrologic data were averaged with a same time base of 10 min. Using the ship as the sampling platform, occasional sampling of the plume of the internal engine was inevitable, especially when the ship was stopped for other research. The air samples may be potentially contaminated with wind direction within a sector of $180^\circ \pm 60^\circ$ relative to the ship's bow and ship speed less than one point five Knot. Some data were excluded based on wind direction and the stop point. It was reported that both $\text{CO}/\text{O}_3 > 15$ and $\text{O}_3 < 8$ ppb⁴ may indicate contamination by ship emission itself. The screened data for CHINARE 2012 were further examined by this criteria. Fortunately, our data fall out of this range, implying that the influence of the exhaust from (R/V) *Xuelong* was minimal.

- Schroeder, W. H. & Munthe, J. Atmospheric mercury—an overview. *Atmos. Environ.* **32**, 809–822 (1998).
- Slemr, F., Brunke, E., Ebinghaus, R. & Kuss, J. Worldwide trend of atmospheric mercury since 1995. *Atmos. Chem. Phys.* **11**, 4779–4787 (2011).
- Slemr, F., Schuster, G. & Seiler, W. Distribution, speciation, and budget of atmospheric mercury. *J. Atmos. Chem.* **3**, 407–434 (1985).
- Sommar, J., Andersson, M. & Jacobi, H.-W. Circumpolar measurements of speciated mercury, ozone and carbon monoxide in the boundary layer of the Arctic Ocean. *Atmos. Chem. Phys.* **10**, 5031–5045 (2010).
- Xia, C., Xie, Z. & Sun, L. Atmospheric mercury in the marine boundary layer along a cruise path from Shanghai, China to Prydz Bay, Antarctica. *Atmos. Environ.* **44**, 1815–1821 (2010).
- Kim, K.-H. *et al.* Atmospheric mercury concentrations from several observatory sites in the Northern Hemisphere. *J. Atmos. Chem.* **50**, 1–24 (2005).
- Cole, A. & Steffen, A. Trends in long-term gaseous mercury observations in the Arctic and effects of temperature and other atmospheric conditions. *Atmos. Chem. Phys.* **10**, 4661–4672 (2010).
- Schroeder, W. *et al.* Arctic springtime depletion of mercury. *Nature* **394**, 331–332 (1998).
- Kaleschke, L. *et al.* Frost flowers on sea ice as a source of sea salt and their influence on tropospheric halogen chemistry. *Geophys. Res. Lett.* **31**, 16114 (2004).
- Pratt, K. A. *et al.* Photochemical production of molecular bromine in Arctic surface snowpacks. *Nat. Geosci.* **6**, 351–356 (2013).
- Lindberg, S. E. *et al.* Dynamic oxidation of gaseous mercury in the Arctic troposphere at polar sunrise. *Environ. Sci. Technol.* **36**, 1245–1256 (2002).
- Lalonde, J. D., Poulain, A. J. & Amyot, M. The role of mercury redox reactions in snow on snow-to-air mercury transfer. *Environ. Sci. Technol.* **36**, 174–178 (2002).
- Strode, S. A. *et al.* Air-sea exchange in the global mercury cycle. *Glob. Biogeochem. Cycle* **21**, 1017 (2007).
- Mason, R. P. & Sheu, G. R. Role of the ocean in the global mercury cycle. *Glob. Biogeochem. Cycle* **16**, 1093 (2002).
- Fisher, J. A. *et al.* Riverine source of Arctic Ocean mercury inferred from atmospheric observations. *Nat. Geosci.* **5**, 499–504 (2012).
- Soerensen, A. L., Skov, H., Jacob, D. J., Soerensen, B. T. & Johnson, M. S. Global concentrations of gaseous elemental mercury and reactive gaseous mercury in the marine boundary layer. *Environ. Sci. Technol.* **44**, 7425 (2010).
- Rigét, F. *et al.* Temporal trends of Hg in Arctic biota, an update. *Sci. Total Environ.* **409**, 3520–3526 (2011).
- Castello, L. *et al.* Low and Declining Mercury in Arctic Russian Rivers. *Environ. Sci. Technol.* **48**, 747–752 (2014).
- Lindberg, S. *et al.* A synthesis of progress and uncertainties in attributing the sources of mercury in deposition. *AMBIO: J. Human Environ.* **36**, 19–33 (2007).
- Aspmo, K. *et al.* Mercury in the atmosphere, snow and melt water ponds in the North Atlantic Ocean during Arctic summer. *Environ. Sci. Technol.* **40**, 4083–4089 (2006).
- Andersson, M., Sommar, J., Gårdfeldt, K. & Lindqvist, O. Enhanced concentrations of dissolved gaseous mercury in the surface waters of the Arctic Ocean. *Mar. Chem.* **110**, 190–194 (2008).
- Parkinson, C. L. & Comiso, J. C. On the 2012 Record Low Arctic Sea Ice Cover: Combined Impact of Preconditioning and an August Storm. *Geophys. Res. Lett.* **40**, 1–6 (2013).



23. Myers, R. A., Akenhead, S. A. & Drinkwater, K. The influence of Hudson Bay runoff and ice-melt on the salinity of the inner Newfoundland Shelf. *Atmos.-Ocean* **28**, 241–256 (1990).
24. Beattie, S. *et al.* Total and Methylated Mercury in Arctic Multiyear Sea Ice. *Environ. Sci. Technol.* **48**, 5575–5582 (2014).
25. Sherman, L. S. *et al.* Mass-independent fractionation of mercury isotopes in Arctic snow driven by sunlight. *Nat. Geosci.* **3**, 173–177 (2010).
26. Mason, R., Rolffhus, K. A. & Fitzgerald, W. Mercury in the North Atlantic. *Mar. Chem.* **61**, 37–53 (1998).
27. Emmerton, C. A. *et al.* Mercury export to the Arctic Ocean from the Mackenzie River, Canada. *Environ. Sci. Technol.* **47**, 7644–7654 (2013).
28. Andren, A. W. & Harriss, R. C. Observations on the association between mercury and organic matter dissolved in natural waters. *Geochim. Cosmochim. Acta* **39**, 1253–1258 (1975).
29. Zhu, J. *et al.* Characteristics of atmospheric total gaseous mercury (TGM) observed in urban Nanjing, China. *Atmos. Chem. Phys.* **12**, 12103–12118 (2012).
30. Pegau, W. S. Inherent optical properties of the central Arctic surface waters. *J. Geophys. Res.* **107**, 8035 (2002).
31. Guéguen, C., Guo, L. & Tanaka, N. Distributions and characteristics of colored dissolved organic matter in the western Arctic Ocean. *Cont. Shelf Res.* **25**, 1195–1207 (2005).
32. Ertel, J. R. *et al.* Dissolved humic substances of the Amazon River system. *Limnol. Oceanogr.* **31**, 739–754 (1986).
33. Allard, B. & Arsenie, I. Abiotic reduction of mercury by humic substances in aquatic system—an important process for the mercury cycle. *Water Air Soil Poll.* **56**, 457–464 (1991).
34. Voelker, B. M., Morel, F. M. & Sulzberger, B. Iron redox cycling in surface waters: effects of humic substances and light. *Environ. Sci. Technol.* **31**, 1004–1011 (1997).
35. Jones, E. P., Anderson, L. G. & Swift, J. H. Distribution of Atlantic and Pacific waters in the upper Arctic Ocean: Implications for circulation. *Geophys. Res. Lett.* **25**, 765–768 (1998).
36. Soerensen, A. L. *et al.* Multi-decadal decline of mercury in the North Atlantic atmosphere explained by changing subsurface seawater concentrations. *Geophys. Res. Lett.* **39**, 1–4 (2012).
37. Eicken, H., Krouse, H. R., Kadko, D. & D.K., P. Tracer studies of pathways and rates of meltwater transport through Arctic summer sea ice. *J. Geophys. Res.* **107**, 8046 (2002).
38. Sander, R. *et al.* Inorganic bromine in the marine boundary layer: a critical review. *Atmos. Chem. Phys.* **3**, 1301–1336 (2003).
39. Kahl, J. D. W., Martinez, D. A. & Zaitseva, N. A. Long-term variability in the low-level inversion layer over the Arctic Ocean. *Int. J. Climatol.* **16**, 1297–1313 (1996).
40. Yu, X. G. The report of 2010 Chinese Arctic Research Expedition. (Ocean Press, Beijing, 2011).
41. Stehr, J. *et al.* Latitudinal gradients in O₃ and CO during INDOEX 1999. *J. Geophys. Res.* **107**, 8016 (2002).
42. Sommariva, R. & von Glasow, R. Multiphase halogen chemistry in the tropical Atlantic Ocean. *Environ. Sci. Technol.* **46**, 10429–10437 (2012).
43. Holloway, T., Levy, H. & Kasibhatla, P. Global distribution of carbon monoxide. *J. Geophys. Res.* **105**, 12123–12147 (2000).
44. Fu, J. *et al.* A regional chemical transport modeling to identify the influences of biomass burning during 2006 BASE-ASIA. *Atmos. Chem. Phys. Discuss.* **11**, 3071–3115 (2011).
45. Geng, F., Zhao, C., Tang, X., Lu, G. & Tie, X. Analysis of ozone and VOCs measured in Shanghai: A case study. *Atmos. Environ.* **41**, 989–1001 (2007).

Acknowledgments

This research was supported by grants from the National Natural Science Foundation of China (Project Nos. 41025020, 41176170), the Program of China Polar Environment Investigation and Assessment (Project No. CHINARE2011–2015), the National Basic Research Program of China (2013CB430000) and the External Cooperation Program of BIC, CAS (Project No.211134KYSB20130012). The authors acknowledge the NOAA Air Resources Laboratory (ARL) for making the HYSPLIT transport and dispersion model available on the Internet (<http://www.arl.noaa.gov/ready.html>).

Author contributions

Z.Q.X. initialed, designed and supervised the study. J.Y., H.K. and Z.L. performed the experiment. L.G.B. provided the meteorological and trace gasses data. C.S. involved the data analysis. J.Y. and Z.Q.X. wrote the manuscript. P.Z. contributed to the discussion of results and manuscript refinement.

Additional information

Supplementary information accompanies this paper at <http://www.nature.com/scientificreports>

Competing financial interests: The authors declare no competing financial interests.

How to cite this article: Yu, J. *et al.* High variability of atmospheric mercury in the summertime boundary layer through the central Arctic Ocean. *Sci. Rep.* **4**, 6091; DOI:10.1038/srep06091 (2014).



This work is licensed under a Creative Commons Attribution-NonCommercial-NoDerivs 4.0 International License. The images or other third party material in this article are included in the article's Creative Commons license, unless indicated otherwise in the credit line; if the material is not included under the Creative Commons license, users will need to obtain permission from the license holder in order to reproduce the material. To view a copy of this license, visit <http://creativecommons.org/licenses/by-nc-nd/4.0/>